cancers

MDPI

Article

Transcriptomic Analyses of MYCN-Regulated Genes in Anaplastic Wilms' Tumour Cell Lines Reveals Oncogenic Pathways and Potential Therapeutic Vulnerabilities

Marianna Szemes [1,*], Zsombor Melegh [2], Jacob Bellamy [1], Ji Hyun Park [1], Biyao Chen [1], Alexander Greenhough [1,3], Daniel Catchpoole [4] and Karim Malik [1,*]

1 Cancer Epigenetics Laboratory, School of Cellular and Molecular Medicine, University of Bristol, Bristol BS8 1TD, UK; jb17872@bristol.ac.uk (J.B.); 2297085p@student.gla.ac.uk (J.H.P.); bc17024.2016@my.bristol.ac.uk (B.C.); Alexander.Greenhough@uwe.ac.uk (A.G.)
2 Department of Cellular Pathology, Southmead Hospital, Bristol BS10 5NB, UK; Zsombor.Melegh@nbt.nhs.uk
3 Department of Applied Sciences, University of the West of England, Bristol BS16 1QY, UK
4 The Kids Research Institute, The Children's Hospital at Westmead, Westmead, NSW 2145, Australia; daniel.catchpoole@health.nsw.gov.au
* Correspondence: M.Szemes@bristol.ac.uk (M.S.); K.T.A.Malik@bristol.ac.uk (K.M.)

Simple Summary: Wilms' tumour (WT) is one of the most common solid paediatric malignancies and arises in the developing kidney. Treatment of most WTs is relatively successful, with the notable exception of tumours with anaplastic histology. Anaplastic WT survival rates can be as low as 30–50%, emphasising the need for a better understanding of their molecular aetiology, in order to facilitate the development of novel therapeutics for poor-prognosis WT. Previous studies have implicated increases in *MYCN* at the DNA and RNA level in WTs with anaplasia, although the biological functions of MYCN protein have not been reported. In this study, we define the expression pattern of MYCN protein in WTs and also modulate MYCN protein levels in anaplastic WT cell-lines to define the functions of MYCN in WT. We show that MYCN depletion leads to decreased cell growth and identify MYCN-regulated genes and pathways that may represent therapeutic vulnerabilities in poor-prognosis WT.

Abstract: The *MYCN* proto-oncogene is deregulated in many cancers, most notably in neuroblastoma, where *MYCN* gene amplification identifies a clinical subset with very poor prognosis. Gene expression and DNA analyses have also demonstrated overexpression of *MYCN* mRNA, as well as focal amplifications, copy number gains and presumptive change of function mutations of *MYCN* in Wilms' tumours with poorer outcomes, including tumours with diffuse anaplasia. Surprisingly, however, the expression and functions of the MYCN protein in Wilms' tumours still remain obscure. In this study, we assessed MYCN protein expression in primary Wilms' tumours using immunohistochemistry of tissue microarrays. We found MYCN protein to be expressed in tumour blastemal cells, and absent in stromal and epithelial components. For functional studies, we used two anaplastic Wilms' tumour cell-lines, WiT49 and 17.94, to study the biological and transcriptomic effects of MYCN depletion. We found that MYCN knockdown consistently led to growth suppression but not cell death. RNA sequencing identified 561 MYCN-regulated genes shared by WiT49 and 17.94 cell-lines. As expected, numerous cellular processes were downstream of MYCN. MYCN positively regulated the miRNA regulator and known Wilms' tumour oncogene *LIN28B*, the genes encoding methylosome proteins PRMT1, PRMT5 and WDR77, and the mitochondrial translocase genes *TOMM20* and *TIMM50*. MYCN repressed genes including the developmental signalling receptor *ROBO1* and the stromal marker *COL1A1*. Importantly, we found that MYCN also repressed the presumptive Wilms' tumour suppressor gene *REST*, with MYCN knockdown resulting in increased REST protein and concomitant repression of RE1-Silencing Transcription factor (REST) target genes. Together, our study identifies regulatory axes that interact with MYCN, providing novel pathways for potential targeted therapeutics for poor-prognosis Wilms' tumour.

Citation: Szemes, M.; Melegh, Z.; Bellamy, J.; Park, J.H.; Chen, B.; Greenhough, A.; Catchpoole, D.; Malik, K. Transcriptomic Analyses of MYCN-Regulated Genes in Anaplastic Wilms' Tumour Cell Lines Reveals Oncogenic Pathways and Potential Therapeutic Vulnerabilities. *Cancers* **2021**, *13*, 656. https://doi.org/10.3390/cancers13040656

Academic Editor: Elizabeth M. Algar
Received: 8 January 2021
Accepted: 1 February 2021
Published: 6 February 2021

Keywords: Wilms' tumour; MYCN; REST; PRMT; TOMM20; RNA-seq

1. Introduction

Wilms' tumour (WT) is the most common paediatric renal malignancy. WT can broadly be categorized as favourable histology (FHWT) or anaplastic. Whilst survival of FHWT patients after neoadjuvant therapy has improved overall survival, patients relapse and experience extensive side-effects as a result of current therapies, with survivors remaining at elevated risk for death long after their diagnosis. Stage III–IV tumours, including anaplastic WT, can have markedly worse prognosis, with a 4-year survival rate as low as ~30–50% for patients will focal or diffuse anaplasia. Thus, there remains a critical requirement for more personalised, targeted therapies to prevent severe illness and death from WT [1,2].

The earliest genetic analyses of WT showed loss-of-function mutations in *WT1* [3,4], missense *TP53* mutations [5] and gain-of-function *CTNNB1* mutations resulting in activation of Wnt signalling [6]. These mutations segregate with WT subtypes; for example, *WT1* and *CTNNB1* mutations in stromal-predominant WT [6], and *TP53* in anaplastic WTs [5,7,8]. More recent genome sequencing studies have found further mutations, including *MYCN*, *REST*, *SIX1/2*, *DROSHA* and *DICER* [7–9], reported in approximately half of all WTs. Inactivating mutations of *REST* were also independently reported, implicating it as a WT tumour suppressor gene in familial and non-familial WT [10].

Together with previous studies demonstrating *MYCN* gain and *FBXW7* loss associated with diffuse anaplasia and poorer outcomes even in the absence of anaplasia, and focal amplifications of *MYCN* in anaplastic WTs [11,12], these whole-genome sequencing analyses suggest an oncogenic role for MYCN in WT. This is further supported by the fact that several groups documented *MYCN* mRNA overexpression in WTs and its association with poor prognosis [13–15]. Together, these strongly implicates *MYCN* deregulation in Wilms' tumorigenesis. However, despite MYCN being known to be important in proliferation of mesenchymal progenitor cells during nephrogenesis [16] and an established oncogenic transcription factor of developmental cancers such as medulloblastoma and neuroblastoma (NB) [17], virtually nothing is known about the biological activities of MYCN in WT, including protein expression patterns, downstream transcriptional targets, and possible pathways regulated.

In this study, we report the first analysis of MYCN protein in primary WTs. Furthermore, our functional analyses demonstrated that MYCN regulates the proliferation of anaplastic WT cell-lines. RNA sequencing of these cell-lines after MYCN depletion identified novel growth control pathways regulated by MYCN, including intersection with the function of the putative WT tumour suppressor gene, *REST* (RE1-Silencing Transcription factor).

2. Materials and Methods

2.1. Wilms' Tumour Cell-Lines, Culture Conditions and siRNA Treatments

The Wit49 [18] and 17.94 [19] anaplastic WT cell-lines were kind gifts from Prof. Herman Yeger and Dr. Keith Brown, respectively. The identity of both cell-lines was confirmed by short tandem repeat (STR) analysis [19,20]. Wit49 cells were cultured at 37 °C under 5% CO_2 in Dulbecco's modified Eagle's medium supplemented with 15% fetal calf serum, 2 mmol/L L-glutamine, 0.1 mg/mL penicillin/streptomycin, 0.6% (*v*/*v*) β-mercaptoethanol and 1× insulin–transferrin–selenium, all purchased from Sigma. 17.94 cells were grown in Dulbecco's modified Eagle's medium supplemented with 10% fetal calf serum, L-glutamine, penicillin and streptomycin. Absence of *Mycoplasma* infection was confirmed by the Mycoalert Mycoplasma Detection Kit (Lonza, Basel, Switzerland).

Knockdown experiments were performed by using RNAiMAX reagent (Invitrogen, Carlsbad, CA, USA) with 20 nM siRNA, according to a reverse transfection protocol,

based on the manufacturer's instructions. Briefly, the siRNA—RNAiMAX mixture was pipetted into the wells of 6-well plates, followed by addition of 2 mL WiT49 cell suspension in antibiotic-free growth medium (70,000 cells/mL), and then mixed gently. Transfections for 17.94 were carried out using the same protocol in 12-well plates, using 150,000 cells/mL medium. Oligonucleotide sequences are shown in Supplementary Table S1.

2.2. Cell Cycle Analysis and Cell Counting

Propidium iodide labelling and fluorescence-activated cell sorting (FACS) analysis was used to detect cell cycle phases. Floating and adherent cells were collected, washed with phosphate-buffered saline (PBS), fixed with ice-cold 70% (*v*/*v*) ethanol and treated with RNase A (Qiagen, Hilden, Germany). After adding 50 µg/mL propidium iodide (Sigma, St. Louis, MO, USA), the samples were incubated at 37 °C for 15 min and analysed on a Fluorescence Activated Cell Sorter LSRFortessaTM X-20 (BD Biosciences, Oxford, UK). About 15,000 events were collected for each replicate, and data were analysed by using FlowJo software. Cell counting was performed by using the Countess automated cell counter (Invitrogen) and trypan blue staining.

2.3. Immunohistochemistry

Tissue microarrays, containing 33 pre-chemotherapy Wilms' tumour samples and fetal and adult kidney sections were stained by using a MYCN antibody (Proteintech, Manchester, UK 10159-2-AP, Lot No: 18121). Immunohistochemistry staining was scored as positive or negative by a pathologist blinded to the specimens. All human tissues were acquired in compliance with the NSW Human Tissue and Anatomy Legislation Amendment Act 2003 (Australia). Ethics clearances 09/CHW/159 and LNR/14/SCHN/392 were approved by the Sydney Children's Hospital Network Human Research Ethics Committee to construct tissue microarrays (TMAs) and use clinical data, which were deidentified. Immunohistochemistry was performed with a Leica Microsystem Bond III automated machine by using the Bond Polymer Refine Detection Kit (Ref DS9800, Leica, Milton Keynes, UK), followed by the Bond Dab Enhancer (AR9432). The slides were dewaxed with Bond Dewax Solution (AR9222) and heat-mediated antigen retrieval was performed using Bond Epitope Retrieval Solution for 20 min.

2.4. Protein Extraction and Western Blot

Cells were lysed in a radioimmunoprecipitation assay (RIPA) buffer (25 mM Tris-HCl pH 7.6, 150 mM NaCl, 1% NP-40, 1% sodium deoxycholate, 0.1% SDS) and protein concentration was determined by using Micro BCA TM protein assay kit (Thermo Fisher, Waltham, MA, USA). Protein extracts were loaded onto SDS polyacrylamide gels and run in a 1× Tris-glycine SDS buffer. After transfer onto a PVDF membrane (Merck Millipore, Watford, UK) by a wet protocol (Bio-Rad, Kidlington, UK), the membrane was blocked in 5% (w/v) skimmed milk, and incubated with the primary antibody solution at 4 °C overnight and horseradish peroxidase (HRP)-labelled secondary antibody solution the next day. Proteins were visualised by using KPL Lumiglo ECL reagent (Insight Biotechnology, Wembley, UK) and X-ray films. The antibodies used are listed in Supplementary Table S2. Western blot image data were quantified by using ImageJ software (http://imagej.nih.gov/ij/). Target protein band density was normalised to the respective loading control and to the normalised intensity of the control sample.

2.5. RNA Extraction, Reverse Transcription and qPCR

RNA was extracted by using the miRNeasy kit (Qiagen), according to the manufacturer's instructions. RNAs were treated with on-column DNase digestion using RNase-free DNase (Qiagen). RNA was transcribed with Superscript IV (Invitrogen) using a mixture of oligodT and random hexamer primers. Quantitative PCR was performed by using the QuantiNova kit (Qiagen) on a Stratagene Mx3500P real-time PCR machine (Agilent,

Cheadle, UK). The housekeeping gene *TBP* was used as a normalising control. Relative gene expression was calculated using the ΔΔCt method; $-\log_2$ fold changes between MYCN-depleted and control samples were calculated after normalisation to TBP. The statistical significance of $\log_2$-transformed fold changes in gene expression was evaluated by using two-tailed Student's *t*-tests. The oligonucleotide primers used in this study are shown in Table S1.

2.6. RNA-seq and Bioinformatic Analysis

Wit49 and 17.94 cells were treated with MYCN-targeting and control siRNAs for 48 hours and were subsequently harvested in Qiazol (Qiagen). RNA was extracted by using the miRNeasy Kit (Qiagen). RNA concentration and quality were checked by using a Nanodrop spectrophotometer and a Bioanalyzer (Agilent). Libraries were prepared from 200 ng RNA and were sequenced by using the paired-end option with 100 bp reads on BGIseq-500 (BGI Genomics, Shenzhen, China). The reads were aligned to the human genome (hg38) by using STAR and the alignment files (BAM) files were further analysed in SeqMonk v1.47. (https://www.bioinformatics.babraham.ac.uk/projects/seqmonk/). Gene expression was quantified by using the Seqmonk RNA-seq analysis pipeline and differentially expressed genes (DEGs) were identified by DESEQ2 ($p < 0.05$). A minimum shrunk fold difference threshold (a conservative corrected value of fold change taking confidence into account) of 1.2 was applied. RNA sequencing data are available from the European Nucleotide Archive (ENA) under the accession number ERP125499. Gene signature enrichment analyses (GSEAs) were performed on pre-ranked lists of $\log_2$-transformed, shrunk fold difference gene expression values (https://www.gsea-msigdb.org/gsea/). Variant analysis was performed using Snippy on the Galaxy platform (https://usegalaxy.org) and the effects of the detected variants were analysed by using the Ensembl Variant Effector Predictor (VEP). Gene expression analysis of published Wilms' tumour datasets and K-means clustering were performed by using the R2 Genomics Analysis and Visualization Platform (http://r2.amc.nl).

2.7. Statistical Analysis

Statistical analysis of quantitative PCR data was performed on $\log_2$-transformed fold change values by using two-tailed Student's *t*-tests. Gene set enrichment analysis of RNA-seq data were evaluated based on normalised enrichment score (NES) and false discovery rate (FDR), which were calculated based on the permutation of genes with a rank score of $\log_2$ fold change expression over the control. Differentially expressed genes (DEGs) in MYCN-depleted Wilms' tumour cells, detected by using RNA-seq, were assessed using the statistical model implemented in DESEQ2. The significance of correlations between clusters of the TARGET-WT data and clinical correlates was assessed by using the Chi-square test. Differential expression of genes and metagenes, which represent gene signatures, among groups of WT and fetal kidney tissue was evaluated by using ANOVA.

3. Results and Discussion

3.1. MYCN Protein Is Overexpressed in the Blastemal Component of Wilms' Tumour and Promotes Proliferation in Wilms' Tumour Cells

Overexpression of *MYCN* mRNA has been reported in poor-prognosis Wilms' tumour [13–15,21] but the prevalence and pattern of MYCN protein expression in Wilms' tumours have, to our knowledge, never been published. Therefore, we performed MYCN immunohistochemistry (IHC) on tissue microarrays (TMAs) containing 33 pre-chemotherapy WT sections (Figure 1). As a normal control, we used a section of a fetal kidney, derived from a 13-week old fetus, as well as a healthy adult kidney. MYCN was detected in 14 tumours, exclusively in the blastemal component. It was localised mostly to the nucleus, but we also detected cytoplasmic staining, with three tumours displaying cytoplasmic staining only. In contrast, in the normal fetal kidney, MYCN was detected solely in

the distal tubules but not in the blastema, while MYCN protein was completely absent from the adult kidney (Figure S1A). While the functional significance of cytoplasmic MYCN protein is not clear, we note that Shoji et al. identified Myc-nick, a cytoplasmic antiapoptotic protein generated from MYCN protein by proteolytic cleavage [22]. Furthermore, localization of MYCN protein was shown to change from nuclear to cytoplasmic during neuronal differentiation [23]. These reports alluded to possible cytoplasmic roles for MYCN protein that remain to be assessed. We also detected MYCN protein in the nuclear and cytoplasmic fractions in both cell-lines, in agreement with our findings in tumours (Figure S1B). Although the number of tumours precluded statistical analysis, our data demonstrates, for the first time, that MYCN protein is expressed in the blastemal cells of Wilms' tumours.

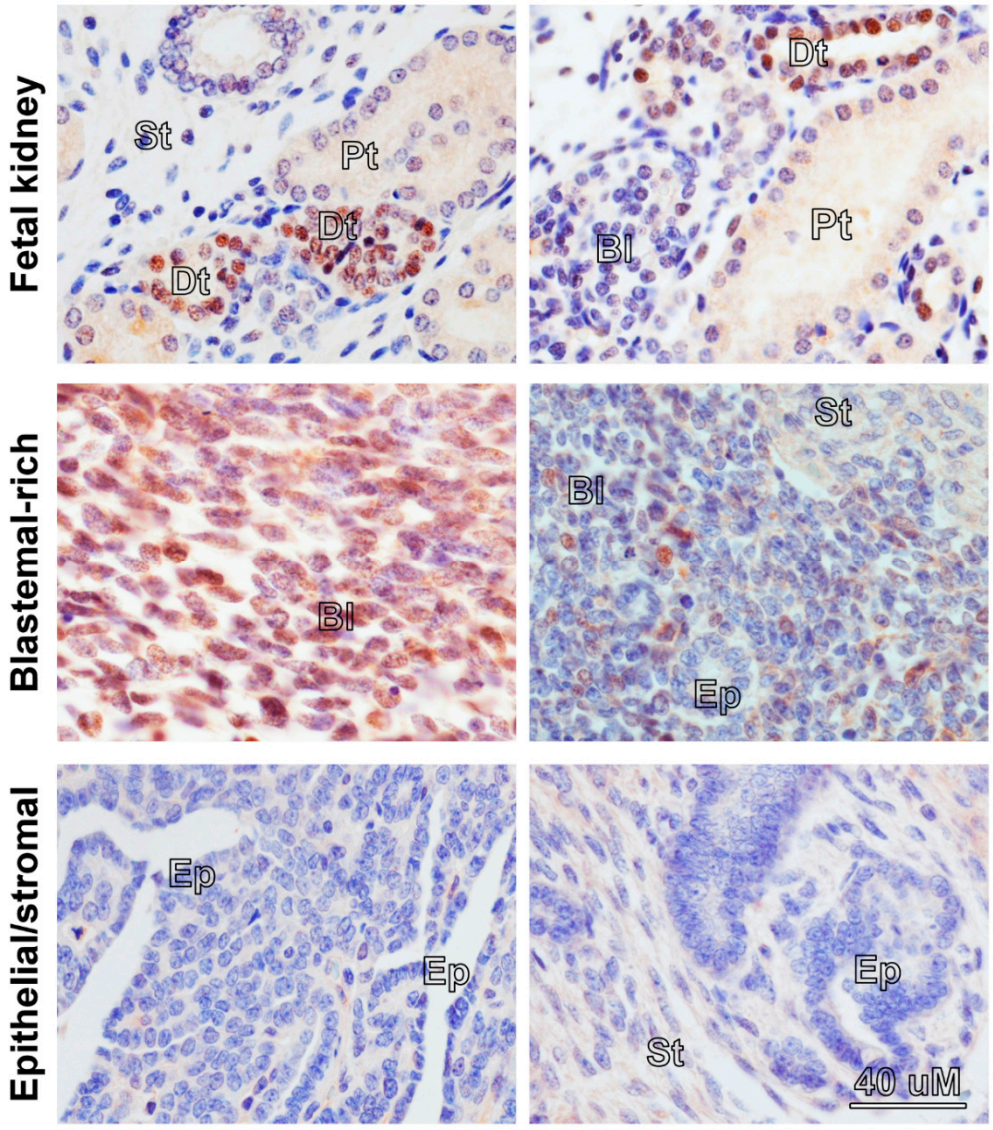

Pre-Treatment WT	Nuclear+	Cyto Only+	Neg	Total
Triphasic WT	7	3	12	22
Blastemal WT	2		3	5
Epithelial WT			1	1
Blastemal and stromal	1			1
Blastemal and epitheloid			1	1
Spindle cell variant WT	1			1
Not specified			2	2
Total	11	3	19	33

Figure 1. Immunohistochemistry in fetal kidney and Wilms' tumours (WT) reveals a blastemal expression for MYCN protein in tumours. All images were taken at the same magnification. MYCN expression was detected in the distal tubules (Dt) in a 13-week-old fetal kidney, while the blastema (Bl), stroma (St) and proximal tubules (Pt) were negative. Blastemal-rich WT showed positivity in the blastemal component. Epithelial (Ep) and stromal structures did not show any expression of MYCN protein. A table summarizing positive MYCN staining in the nucleus or the cytoplasm only in WT, according to histology, is shown underneath.

To characterize the effect of MYCN on the growth of Wilms' tumour cells, we knocked it down in two anaplastic WT cell-lines, Wit49 and 17.94 (Figure 2). After 120 h of MYCN depletion by two independent MYCN-targeting siRNAs, there was a substantial and significant reduction in live cell counts ($p < 0.01$). The number of dead cells did not increase, suggesting that the decrease in live cells was due to growth inhibition rather than increased cell death. To investigate the effect of MYCN depletion on the cell cycle, we performed a cell cycle analysis on Wit49 (Figure S2). MYCN knockdown by either siRNA led to a significant reduction of cells in the S phase, while the proportion of cells in G2/M increased significantly ($p < 0.01$), indicative of a G2/M arrest. There was no increase of cells in the sub-G1 phase, in agreement with our previous observation of no increase in dead cell counts. These studies suggest that MYCN primarily exerts control over WT proliferative pathways as opposed to apoptosis and cell survival.

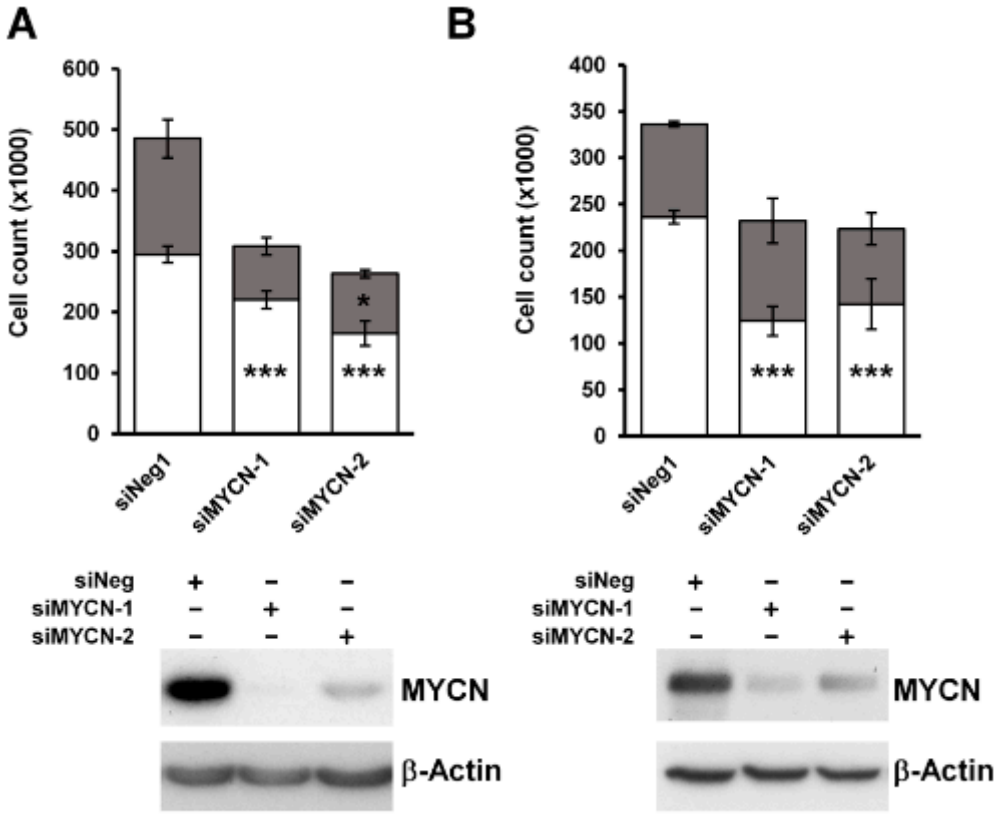

Figure 2. MYCN depletion leads to significant growth inhibition in anaplastic WT cell-lines. (**A**) MYCN depletion resulted in significant growth suppression after 120 h of treatment in Wit49, but not in an increase in dead cells, using two different siRNAs. ($n = 3$, *** $p < 0.01$, * $p < 0.05$, two-tailed *t*-tests). Live cell counts are indicated by white bars and dead cell counts are shown in grey. (**B**) MYCN knockdown also led to significant growth suppression in 17.94 cells after 120 h ($n = 3$). Western blotting confirmed efficient knockdown of MYCN protein in both cell-lines. * Uncropped Western blots are available in Figure S5A.

3.2. MYCN-Regulated Gene Signatures in Wilms' Tumour Reveal Downstream Growth-Regulatory Pathways

To identify MYCN-regulated genes in Wilms' tumour, we performed RNA-seq of both anaplastic WT cell-lines following MYCN knockdown (Supplementary Figure S3A). MYCN-regulated genes were defined as differentially expressed genes (DEGs) that had a significant ($p < 0.05$) and substantial change (minimum shrunk fold change, a corrected value based on confidence, of 1.2) in their expression levels, as assessed by using DESEQ2. We found 1060 upregulated genes in Wit49 and 396 in 17.94, with a highly significant overlap of 212 genes between the two cell-lines ($p < 10^{-10}$) (Figure 3A). There were 349 downregulated genes shared by the two cell-lines, with 1086 and 699 identified in Wit49 and 17.94, respectively ($p < 10^{-10}$). The shared 561 MYCN-regulated genes in WT are shown in Supplementary Table S3 and Figure S3B. Known MYCN target genes, and genes related to WT or kidney development are highlighted on the heatmap (Figure 3B) Our RNA sequencing confirmed the previously characterized *TP53* mutations in the Wit49 and 17.94 cell-lines, and we identified a known polymorphic variant in *REST* in Wit49. We also confirmed the absence of mutations in other WT candidate genes, including MYCN (Supplementary Table S4). A panel of the DEGs identified by RNA-seq after MYCN knockdown were validated in both cell-lines by qPCR. We confirmed downregulation of *LIN28B*, a MYCN target gene in neuroblastoma [24], both at the RNA (Figure 3C) and protein level (Supplementary Figure S3B). LIN28B is an established regulator of nephrogenesis, promoting expansion of the progenitor pool, and a direct oncogenic driver in WT [25,26]. LIN28B suppresses *let-7* miRNAs but can also influence gene expression via other mechanisms, including regulation of translation [27]. Therefore, MYCN is likely to exert control at the post-transcriptional as well as the transcriptomic level.

Amongst the novel genes, one of the biggest expression changes was the *ROBO1* gene, which increased over fourfold after MYCN knockdown in both WT cell-lines (Figure 3C). *ROBO1* encodes the transmembrane Roundabout Guidance Receptor 1 involved in SLIT/ROBO signalling, a key developmental pathway [28]. *Robo1* is a tumour suppressor gene in other cellular systems, with *Robo1* knockout mice being predisposed to lung adenocarcinomas and lymphomas [29]. Other studies have indicated that Slit/Robo signalling is required for normal kidney development [30], and *Robo1* expression increases in the pretubular aggregates compared with the metanephric mesenchyme, implying a role for Robo1 in early renal differentiation [31]. We also note that *SLIT2* is frequently epigenetically silenced in WTs [32], further supporting a tumour-suppressive role for SLIT/ROBO signalling in WT.

Gene set enrichment analysis indicated that MYCN repressed kidney differentiation and developmental genes (Supplementary Figure S3C). To study how MYCN influences cell differentiation during nephrogenesis, we queried gene signatures characteristic of different cell populations in the fetal kidney determined by Menon et al. by using single cell RNA-seq [33]. We found that MYCN-activated genes were overexpressed in proliferating cells, while gene signatures of both podocytes and stromal cells were repressed by MYCN, consistent with a role for MYCN in promoting growth and repressing differentiation (Supplementary Figure S3D). *COL1A1,* a marker gene for stromal cells, was upregulated more than two-fold in our RNA-seq data after MYCN depletion. Moreover, COL1A1 protein is documented to be significantly downregulated in anaplastic WT compared with favourable histology WT [34].

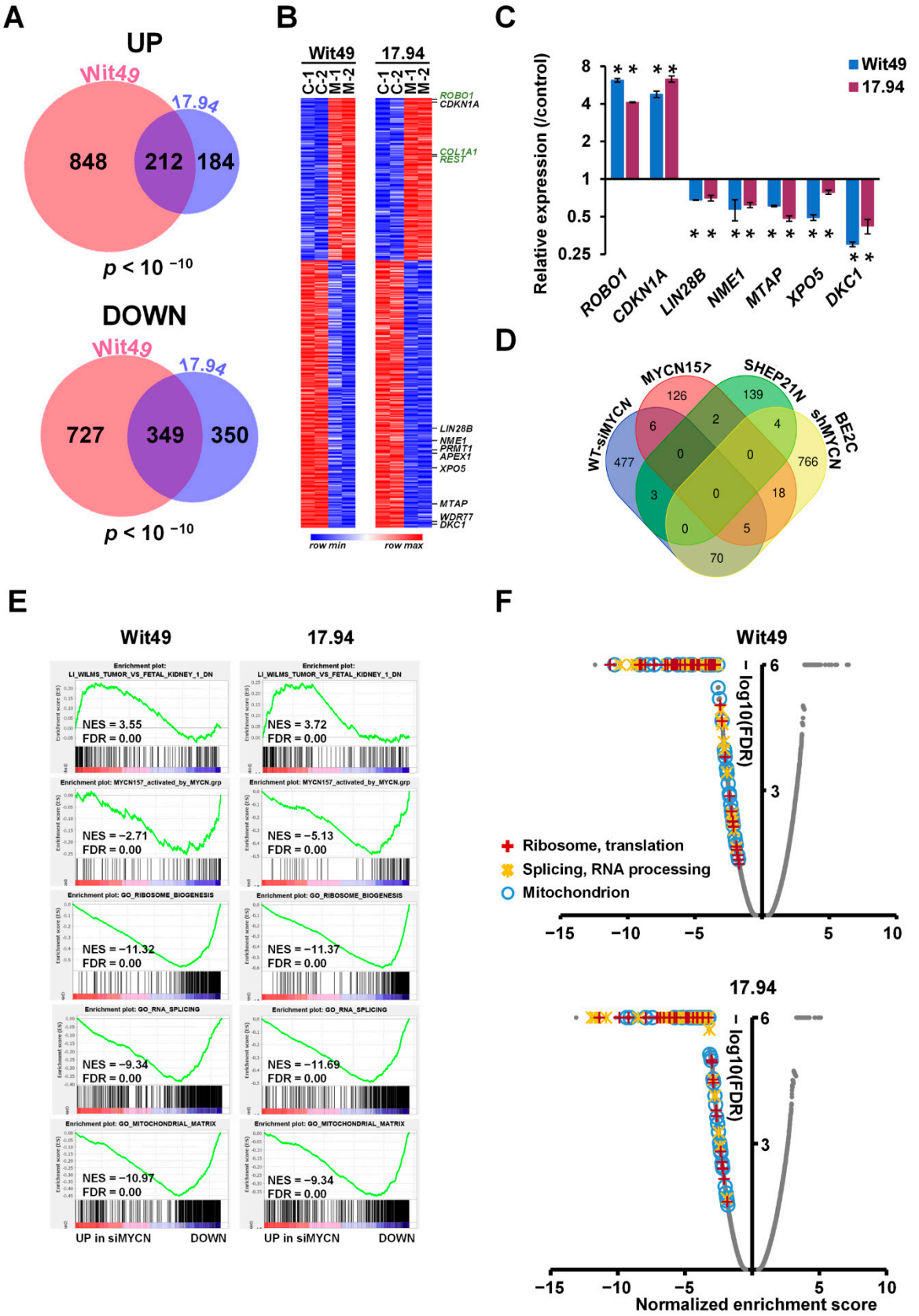

Figure 3. Genes and pathways identified by RNA-seq in MYCN-depleted anaplastic WT cells. (**A**) Venn diagrams showing highly significant overlaps between differentially expressed genes (DEGs) in Wit49 and 17.94 after MYCN depletion for 48 h, for up- and downregulated genes. DEGs were determined as statistically significant ($p < 0.05$) and having a minimum shrunk fold change (a conservative corrected value) of 1.2, calculated by using DESEQ2. The probability values for shared genes are indicated. (**B**) Heatmap of shared 561 DEGs in Wit49 and 17.94. Expression data of replicate control samples are

indicated as C-1 and C-2, while those of MYCN depleted samples are shown as M-1 and M-2. Examples of known MYCN target genes are shown in black, while genes associated with kidney development or Wilms' tumour predisposition are highlighted in green. (**C**) Validation of identified select MYCN-regulated genes in WT cells by qPCR, 48 h after MYCN knockdown. A representative of three biological replicates is shown. Significance was calculated based on the biological replicates (* $p < 0.05$, *t*-tests). (**D**) Venn diagram showing overlaps of MYCN-regulated genes in WT described in this study, with MYCN target genes identified in neuroblastomas. (**E**) GSEA plots showing upregulation of gene signatures repressed in WT as compared to fetal kidney, upon depletion of MYCN. MYCN-activated genes of the MYCN157 signature, identified in NB, were downregulated. Examples of gene set enrichment analysis (GSEA) of downregulated Gene Ontology (GO) gene sets associated with ribosomal and mitochondrial function and splicing in MYCN-depleted WT cells are also shown. (**F**) Volcano plots of gene set enrichment analysis on MYCN depletion transcriptomes in WT cells. Normalised enrichment scores and false discovery rates (FDR) were calculated. Gene Ontology gene categories indicated universal downregulation of gene sets linked to ribosomal and mitochondrial function, as well as those associated with RNA processing and splicing. Scores of all gene sets are shown in grey, while those of statistically significant gene sets (FDR < 0.05) in the highlighted functional categories are indicated according to the legend.

MYCN targets have been extensively studied in NB and several target lists have been described. We compared our WT-specific MYCN targets with some identified by transcriptomic and chromatin immunoprecipitation analyses in NB, specifically (i) the MYCN157 signature, derived from IMR32 cell-line DEGs following MYCN knockdown, subsequently filtered by correlation with MYCN mRNA expression in primary NBs [35]; (ii) DEGs from a MYCN-overexpressing isogenic model [36] and (iii) genes bound by MYCN and correlated with MYCN in the SEQC NB expression dataset (GSE49712) [37] (Figure 3D). We found surprisingly little overlap of our top DEGs with these NB-specific MYCN targets, emphasising the importance of cellular context. To characterise the function of the newly identified MYCN regulated genes, we performed a Gene Ontology (GO) enrichment analysis (Table S5). The most highly enriched component was the "RNA nuclear export complex" (GO:0042565), including *XPO5* and *RAN*, which is responsible for the transport of pre-miRNAs from the nucleus, suggesting that MYCN may substantially alter the miRNA profile in the cytoplasm. Mutations in *DICER* and *DROSHA*, key enzymes in microRNA biogenesis, were previously shown to be involved in WT pathogenesis [8]. The WT-specific MYCN-regulated genes were also enriched in GO categories related to mitochondrial, ribosomal, spliceosomal and methylosome complexes and telomere maintenance, emphasising the control of several major cellular processes by MYCN.

To obtain an extended global overview of the transcriptional control of MYCN in WT, we performed gene set enrichment analyses (GSEA) with the DEGs from Wit49 and 17.94 cell-lines. GSEA revealed that MYCN knockdown led to activation of genes downregulated in WT relative to fetal kidney (Figure 3E) [38], and repression of genes elevated in WT relative to the fetal kidney (Figure S4A). Thus, MYCN knockdown reverses, at least in part, the WT-specific signature.

MYCN-activated genes in the MYCN157 signature were significantly downregulated, showing regulation of the NB-specific target genes in WT cells, despite the minimal overlap of our top DEGs (with the biggest or most significant changes) with the top MYCN targets in NB. Similarly, several MYC target gene sets were downregulated in both cell-lines, indicating that MYCN drives canonical MYC target genes in WT (Figure S4B), like the curated MYC gene set in Hallmark [39]. Further, genes encoding mitochondrial proteins that were recently shown to be regulated by MYCN [40] were also downregulated, emphasizing the role of MYCN in activating mitochondrial function genes in WT. Genes encoding for proteins with roles in "RNA export from nucleus" were downregulated, which may affect pre-miRNA transport and the miRNA pool in the cytoplasm, while those participating in "Unfolded protein response" were upregulated, suggestive of endoplasmic reticulum stress in the MYCN-depleted cells (Figure S4C).

Gene signatures related to ribosomal biogenesis, splicing and mitochondria were all found to be downregulated following MYCN knockdown, reinforcing the results of the GO analysis with shared WT-specific MYCN-regulated genes (Figure 3E). In fact, all the

gene ontology signatures related to ribosomal function, RNA processing/splicing and mitochondria were found to be profoundly downregulated in both MYCN-depleted cell lines, suggesting strong activation of these gene expression programmes by MYCN in WT (Figure 3F).

Ribosomal biogenesis was reported to be upregulated in *MYCN*-amplified neuroblastoma too, and inhibitors of RNA polymerase I (which transcribes ribosomal RNA genes) suppressed MYCN expression and promoted apoptosis of *MYCN*-amplified (MNA) NB cells, both in vitro and in vivo [41]. Deregulation of splicing [42] and metabolic reprogramming by MYCN [43] were also observed in neuroblastomas, consistent with our transcriptomic analysis in WT.

To investigate the expression of *MYCN* and its target genes in a large set of primary Wilms' tumour tissues, we analysed the publicly available WT RNA-seq dataset, TARGET-WT (SRP012006), containing expression data for 124 high-risk tumours. We found a strong and highly significant positive correlation between the expression of *MYCN* and its activated target genes in WT ($R = 0.43$, $p = 5.6 \times 10^{-7}$), suggesting a regulatory link in vivo (Figure 4A). The correlation between *MYCN* and the newly identified repressed genes in the tumours was less pronounced and did not reach significance ($R = -0.15$, $p = 0.087$), suggesting that other regulators might also be involved in repression. For example, *LIN28B* was reported to be activated via chromosomal translocation and amplification in WT, independent of MYCN [44], and *REST* can be inactivated via mutations. To identify the tumours with a MYCN-regulated signature and to study their clinical correlates, we clustered the WT transcriptomic dataset according to the expression of the shared 561 MYCN target genes (Figure 4B). Two clusters were identified: a larger group (Cluster 1) with a mostly uniform expression of target genes and a smaller group of 14 tumours (Cluster 2), displaying upregulated and downregulated subsets of our MYCN target genes. The tumours in Cluster 2 were generally at higher stages, with a significant difference in distribution (Chi-squared test $p = 0.015$, Figure 4C). Cluster 1 contained all the Stage 1 tumours, and the proportion of Stage 2 ones was higher as well (43% vs. 14%). In contrast, there was a higher proportion of Stage 3 and 3B tumours in Cluster 2: 71% vs. 28% and 7% vs. 3%, respectively. Patients with tumours in the MYCN-regulated group (Cluster 2) had lower survival (42.9% vs. 61.8%), although this trend did not reach significance, probably because of the relatively low number of patient samples in Cluster 2 (Figure 4D).

To evaluate the expression of functional gene sets in primary Wilms' tumours, we assessed the overall expression of GO gene categories highlighted by our RNA-seq analysis, represented as metagenes, in the newly defined clusters in TARGET-WT (Figure 4E). Ribosomal genes had significantly and substantially higher expression in Cluster 2 than in Cluster 1 ($p = 3.2 \times 10^{-15}$). Genes coding for mitochondrial protein complexes ($p = 3.8 \times 10^{-13}$) and methylosome components ($p = 4.7 \times 10^{-8}$) were similarly significantly upregulated in Cluster 2, reinforcing our data in WT cell-lines. Together, these analyses show that the DEGs we identified in the Wit49 and 17.94 cell-lines correlated with MYCN in primary WTs, and that pathways identified by our in vitro analyses were aberrant in a subset of higher-stage WTs.

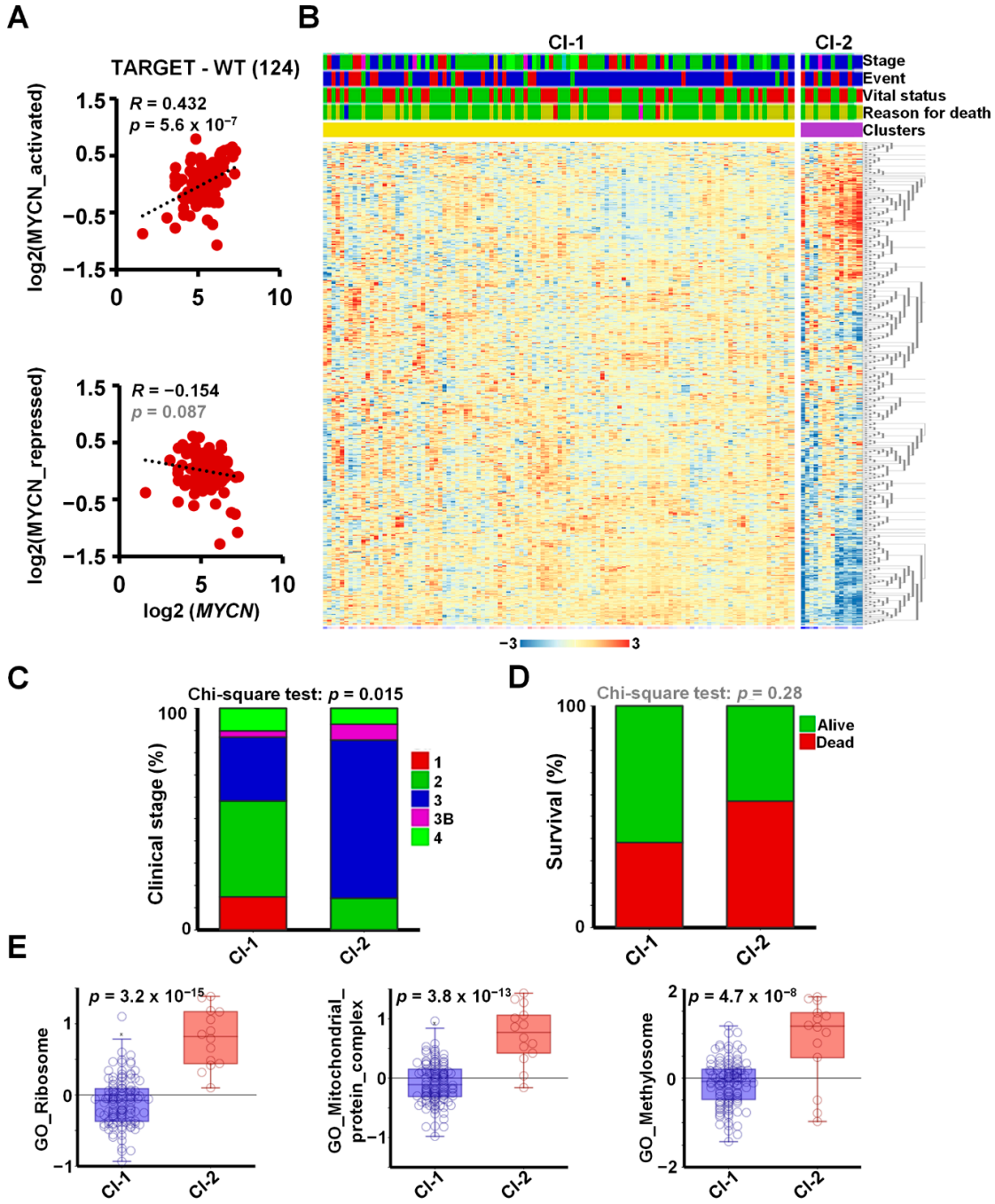

Figure 4. Meta-analysis of MYCN-regulated genes in the WT-TARGET dataset identifies distinct patient clusters. (**A**) Overall expression of MYCN-activated genes, identified as shared downregulated hits in MYCN-depleted WT cells, showed a strong and significant positive correlation with MYCN expression in the TARGET-WT dataset (SRP012006), containing transcriptomic data of 124 high-risk WTs. Overall expression of MYCN-repressed genes displayed a modest inverse correlation that did not reach significance. (**B**) K-means clustering (K = 2) performed on the TARGET-WT dataset based on the expression of 561 MYCN-regulated genes in WT, identified in this study. Clinical information is shown as coloured bars on the top: stage (red = 1, green = 2, blue = 3, magenta = 3b, yellow = 4, black = 5_3B, turquoise = 5_4), event type (none = red, blue = relapse, green = progression), vital status (green = alive, red = dead) and reason for death (green = none, yellow = tumour, red = infection, blue = toxicity, magenta = tumour and toxicity). (**C**) Proportion of tumours with various clinical stages. Chi-square tests showed that the association of clinical stages with clustering according to MYCN-regulated genes was significant. Stages represented by a single tumour were omitted. (**D**) More death occurred in patients with tumours in Cluster 2; however, this association did not reach significance. (**E**) Overall expression of genes encoding for the ribosome, mitochondrial protein complexes and methylosome components was significantly higher in Cluster 2 tumours as compared with those in Cluster 1 (ANOVA).

3.3. MYCN Upregulates the Key Mitochondrial Transporter Gene TOMM20, Overexpressed in Blastemal and Relapsed WT

Gene set enrichment analysis revealed a profound downregulation of genes encoding for mitochondrial complexes upon MYCN depletion in both anaplastic WT cell-lines (Figure 5A). The most downregulated genes included *TOMM20* (Figure 5B), encoding a member of the translocase of the outer membrane (TOM) complex, responsible for the import of newly synthesised mitochondrial proteins from the cytosol. The TOM complex works in close co-operation with the translocase of the inner membrane (TIM) complex [45], a key member of which, *TIMM50*, was also downregulated with MYCN depletion. We confirmed the downregulation of these mitochondrial protein genes together with *PDK1* by qPCR (Figure 5C); PDK1 (Pyruvate Dehydrogenase Kinase 1) is a gatekeeper of the Warburg effect and is frequently overexpressed in cancer [46]. Downregulation of TOMM20 was also confirmed at the protein level in both anaplastic WT lines (Figure 5D). In the TARGET-WT RNA-seq dataset, we observed a significant positive correlation between the expression of *MYCN* and *TOMM20*, consistent with our findings (Figure 5E). *TOMM20* was inferred to be a MYCN target gene in neuroblastoma due to MYCN binding to its promoter and its mRNA positively correlating with MYCN [37]. However, our data at both protein and RNA levels demonstrated, for the first time, that TOMM20 is directly regulated by MYCN. In two other publicly available transcriptomic datasets by Perlman et al. [47,48], *TOMM20* was found to be significantly overexpressed in relapsed vs. non-relapsed WT (Figure 5F) and in blastemal tumours relative to other tumours (Figure 5G). *TOMM20* overexpression is associated with poor prognosis in other cancers such as colorectal cancer and chondrosarcoma [49,50], and TOMM20 knockdown in colorectal cancer cells led to increased mitochondrial damage, significantly reduced ATP production and apoptosis in vitro, and reduced growth of tumour xenografts in vivo. Whilst metabolic defects in WT have not been extensively studied, it has been demonstrated that stromal tumours have markedly reduced mitochondrial mass and function compared with blastemal tumours, and that oxidative phosphorylation is considerably lower in WT than normal kidneys [51]. Taken together with our data, this invokes the possibility that MYCN-regulated overexpression of TOMM20 may alter mitochondrial protein import by the TOM complex and facilitate the glycolytic switch (Warburg effect) in poor-prognosis WT. In this regard, it is interesting to note that TOMM20 overexpression has been demonstrated to retard mitochondrial protein import, presumably by disruption of the normal stoichiometry of subunits of the import receptor complex [52].

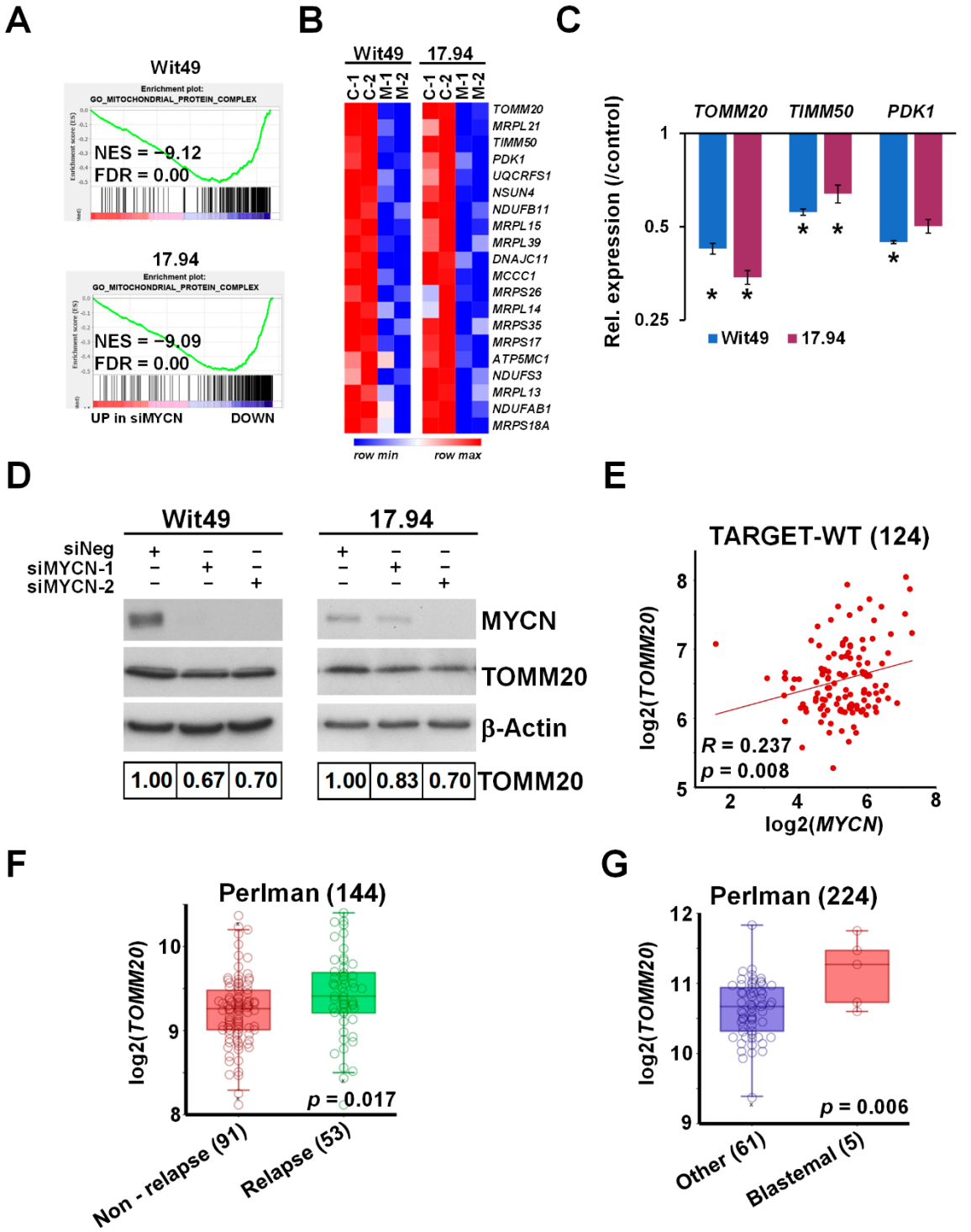

Figure 5. MYCN regulates *TOMM20* and other mitochondrial function genes. (**A**) GSEA showing downregulation of genes encoding for mitochondrial protein complexes with MYCN depletion. (**B**) Heatmap displaying the expression of the top 20 genes in the leading edge of the Gene Ontology (GO) mitochondrial protein complex gene category in MYCN-depleted WT cells. (**C**) Validation of select mitochondrial genes in Wit49 and 17.94 cells by qPCR, 48 h after MYCN knockdown. A representative of three biological replicates is shown. *t*-tests were performed on the biological replicates (* $p < 0.05$). (**D**) Western blot and quantification showing the reduction of TOMM20 protein expression after 72 h of MYCN depletion. ($n = 3$). (**E**) Expression of *MYCN* and *TOMM20* genes was significantly correlated in the TARGET-WT dataset (SRP012006). (**F**) Relapsed WTs had significantly higher expression of *TOMM20* mRNA than non-relapsed ones, as detected in GSE10320. (**G**) *TOMM20* was also more highly expressed in blastemal WTs than in tumours with other histology (GSE31403). Uncropped Western blots are available in Figure S5B.

3.4. MYCN Upregulates Methylosome Components in WT and Influences Post-Translational Regulation by Promoting Arginine Methylation

The methylosome was one of the most enriched GO categories in our transcriptomic analysis of MYCN depletion in WT cells, with 6 out of the 12 members significantly downregulated in both cell-lines. A heatmap of the methylosome genes shows that the other six members were also downregulated, albeit to a lesser extent (Figure 6A). Expression changes of *WDR77*, encoding for MEP50, and *PRMT1* were validated by using qPCR (Figure 6B). Analysis of RNA-seq data indicated that *PRMT5* was also downregulated in both cell-lines, although to a lesser extent.

Downregulation was confirmed at the protein level for three key methylosome components: PRMT1, catalysing asymmetrical arginine di-methylation (ADMA), and PRMT5 and WDR77/MEP50, acting in a complex to effect symmetrical arginine di-methylation (SDMA) modification (Figure 6C). We hypothesized that such profound downregulation of the methylosome components may influence global arginine di-methylation levels, which we tested by using antibodies against ADMA and SDMA modifications. We found that ADMA levels were reduced with MYCN depletion in both cell-lines by using two different siRNAs. SDMA modification was also reduced in the 15–20 kDa size range, suggesting reduction of SDMA marks on snRNP proteins, which participate in RNA splicing.

Our analyses further established that *PRMT1* and *WDR77* were significantly overexpressed in WT as compared with the fetal kidney in the transcriptomic dataset published by Li et al. [38] (Figure 6D), supporting a role for arginine methyltransferases in WT pathogenesis. Both *PRMT1* and *WDR77* are MYCN targets within the MYCN157 gene set for poor prognosis NB [35], and MYCN also binds the *PRMT5* promoter [53]. PRMTs are often overexpressed in cancer [54], and we have previously shown that PRMT5 is a survival factor for MYCN-amplified NB, with PRMT5 interacting with and methylating MYCN protein [55]. We have also shown that neuroblastoma cells are sensitive to PRMT1 inhibition [56]. Small molecule inhibitors of PRMTs have been developed recently and were demonstrated to have efficacy in vitro and in vivo against cancers such as mantle cell lymphoma [57,58], and are currently in clinical trials for solid tumours and various forms of leukaemia [59]. Our transcriptomic and protein level analyses suggest that a PRMT–MYCN axis may also be involved in WT, and that selective inhibition of PRMTs may represent a novel targeted therapy for poor-prognosis WT.

3.5. MYCN Represses the WT Predisposition Gene REST, Leading to Activation of Its Target Genes

Exome sequencing of familial and non-familial Wilms' tumors recently revealed loss-of-function mutations in the *REST* gene (encoding RE1 Silencing Transcription Factor) [10]. REST is a Krüppel-type zinc-finger transcription factor which acts as a repressor of gene transcription via numerous interactions with chromatin modifiers, and deregulation of REST is implicated in the pathogenesis of several diseases, including cancer [60]. Intriguingly, our RNA-seq revealed *REST* as one of the genes upregulated upon depletion of MYCN. De-repression of REST was also confirmed at the protein level in both cell-lines using two different siRNAs (Figure 7A). Furthermore, we found that the REST-repressed target genes *STMN3*, *GDAP1* and *ENAH* were decreased after MYCN knockdown, consistent with the upregulation of functional REST protein (Figure 7B). To query the effect of MYCN on REST-regulated genes in WT, we performed GSEA on our MYCN depletion transcriptomic data using gene signatures established in stem-cell-derived neurons [61] and embryonic stem cells (ESCs) [62] (Figure 7C). Both gene sets were significantly downregulated in both WT cell-lines upon MYCN knockdown, suggesting a MYCN–REST regulatory axis in WT.

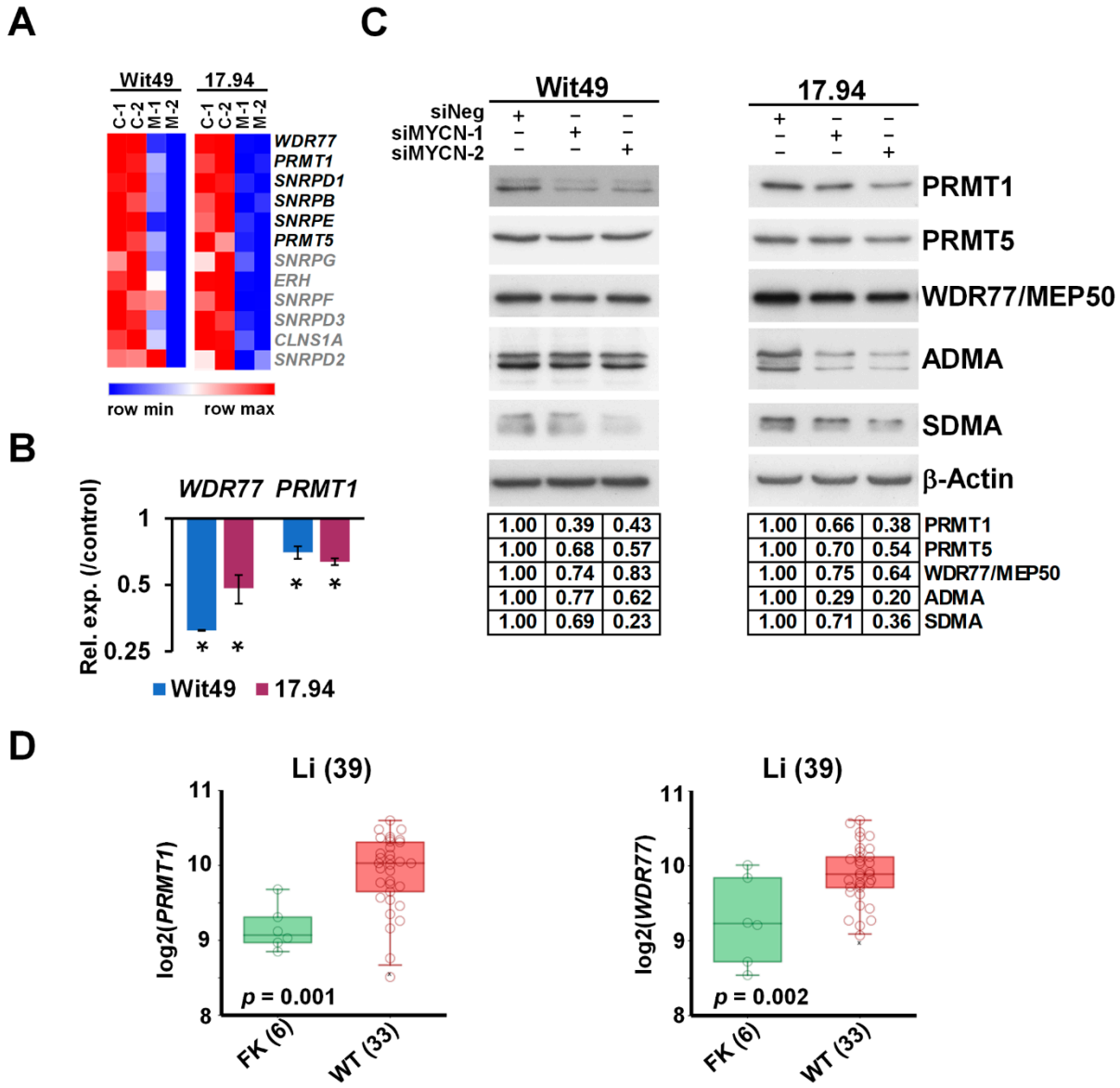

Figure 6. MYCN activates methylosome genes in WT. (**A**) Heatmap of genes encoding for methylosome components, showing expression in MYCN-depleted WT cells. Genes highlighted in black were identified in this study as significantly and substantially regulated by MYCN in two anaplastic WT cells. (**B**) Validation of select methylosome genes in WT cells by qPCR, 48 h after MYCN knockdown. Statistical significance was calculated based on biological replicates, and expression for one representative is shown (* $p < 0.05$). (**C**) Western blot of select methylosome components in WT cells 72 h after MYCN knockdown with two different siRNAs ($n = 3$). Protein expression was calculated based on densitometry and normalised for the loading control on the same filter. Confirmation of MYCN depletion is shown in Figure 5D. (**D**) *PRMT1* and *WDR77*, encoding for MEP50, were shown to be expressed at significantly higher levels in WT than in the fetal kidney (GSE6120). Uncropped Western blots are available in Figure S5C.

REST was found to be significantly repressed in cluster 2 of the TARGET–WT dataset (Figure 7D), which contained tumours with the MYCN signature. In contrast, ESC-specific REST target genes were de-repressed in the same group of tumours, as indicated by the expression of REST target metagenes, representing the overall expression of MYCN-regulated REST genes of the signature described by Johnson et al. [62] (Figure 7E). We also found *REST* was significantly repressed in WT as compared with the fetal kidney in our cohort of primary samples (Figure 7F). Expression of *MYCN* and *REST* showed a strong inverse correlation in these tissues ($R = -0.73$, $p = 0.0003$) (Figure 7G). Thus, our data identify the repression of the presumptive WT tumour suppressor gene *REST* as a hitherto uncharacterised oncogenic pathway downstream of MYCN deregulation.

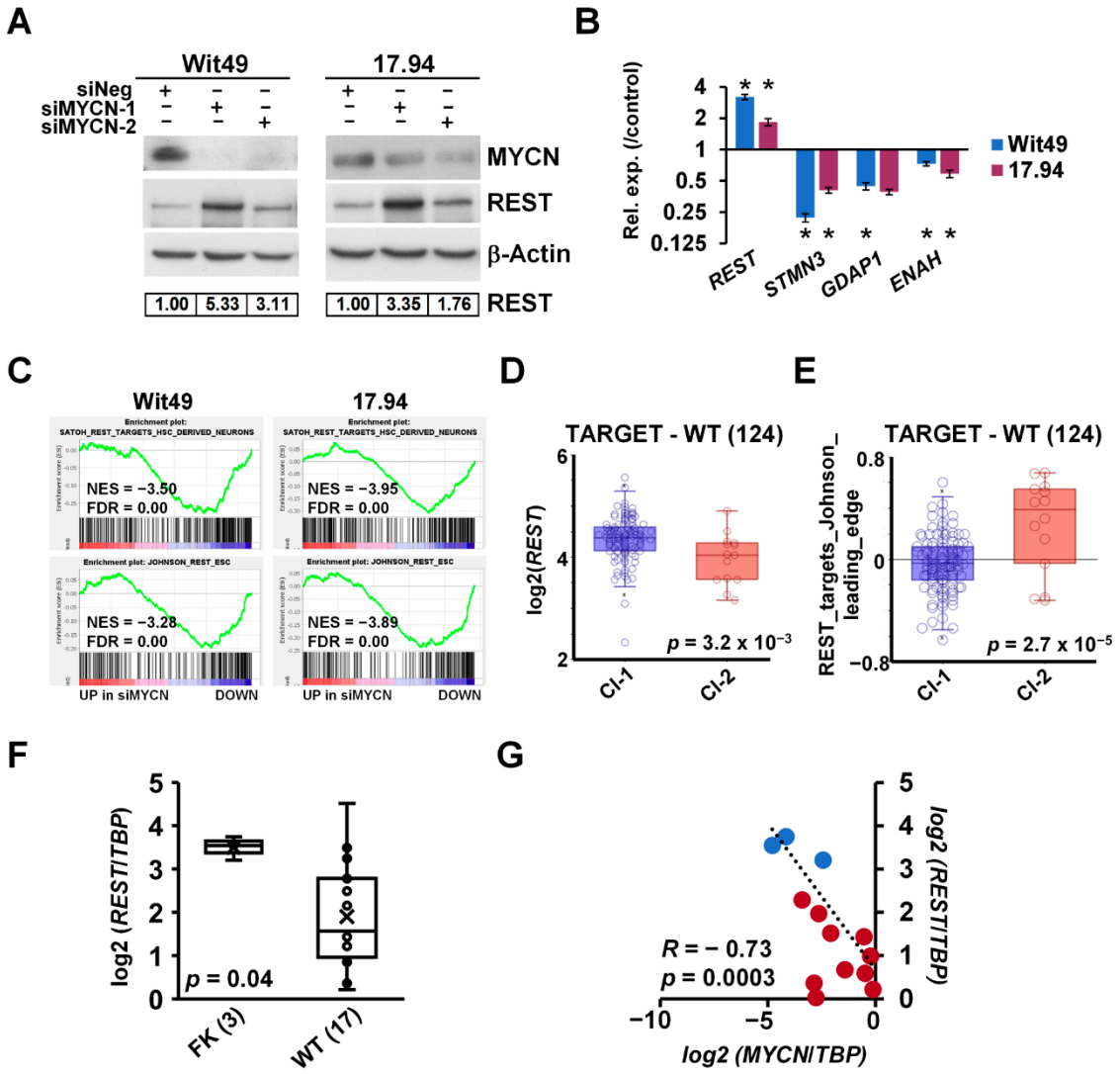

Figure 7. MYCN represses the WT predisposition gene *REST.* (**A**) REST protein is derepressed upon MYCN depletion (n = 3). Protein expression was calculated based on densitometry and normalised for loading control. (**B**) Validation of the upregulation of *REST* mRNA and downregulation of its target genes by qPCR after MYCN depletion for 48 h (n = 3). A representative experiment is shown. *t*-tests were performed on biological replicates (* $p < 0.05$). (**C**) GSEA showed downregulation of REST target genes with MYCN depletion. (**D**) REST has a significantly lower expression in Cluster 2 tumours in the TARGET-WT dataset (SRP012006) as compared with Cluster 1 (ANOVA). (**E**) REST target genes, showing a significant overall overexpression in Cluster 2 WT as compared with Cluster 1. (ANOVA) (**F**) *REST* was found to be significantly repressed in WT as compared with FK by qPCR, as assessed by a *t*-test. (**G**) Expression of *MYCN* and *REST* was highly and significantly correlated in WT and FK, indicated by red and blue dots, respectively. Uncropped Western blots are available in Figure S5D.

Taken together, this study demonstrates that MYCN promotes growth and survival in WT by regulating multiple genes affecting splicing, translation, post-translational modification, microRNAs, metabolism and cellular differentiation (Figure 8). The intersection of MYCN with co-operative oncogenic and tumour suppressor pathways represent possible vulnerabilities of poor-prognosis Wilms' tumour which can be exploited in the future for urgently required targeted therapeutics.

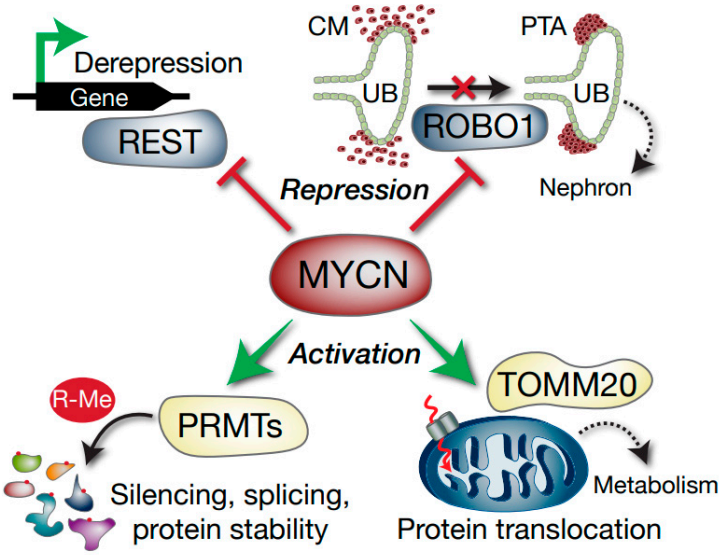

Figure 8. Model depicting select Wilms' tumour MYCN targets with potential functional consequences. MYCN represses the *REST* tumour suppressor gene, which can result in activation of REST-repressed genes. *ROBO1* is also repressed, which may compromise the differentiation of the condensing mesenchyme (CM) into pre-tubular aggregates (PTA) via inhibition of SLIT–ROBO developmental signalling. The ureteric bud (UB) is also shown. MYCN activation of methylosome genes such as PRMTs alters arginine methylation (R-Me), with subsequent alterations in functions including mRNA splicing and protein stability. Activation of *TOMM20* by MYCN may lead to aberrant mitochondrial protein translocation (dashed red arrow) and altered tumour cell metabolism.

Supplementary Materials: The following are available online at www.mdpi.com/2072-6694/13/4/656/s1. Figure S1. MYCN protein expression., Figure S2. Cell cycle analysis. Depletion of MYCN protein in Wit49 cells by two different siRNAs for 72 hours resulted in a significant increase in the proportion of cells in the G2/M phase and a decrease in the S phase ($n = 3$, *** $p < 0.01$, *t*-test), Figure S3. Western blots of MYCN and LIN28B and GSEA of differentiation gene signatures in WT, Figure S4. GSEA analysis in transcriptomes of MYCN-depleted WT cells, Figure S5. Uncropped images of Western blots; Table S1. Oligonucleotides, Table S2. Antibodies, Table S3. Shared MYCN-regulated genes in Wit49 and 17.94, Table S4. Variant analysis of Wilms' tumour candidate genes in Wit49 and 17.94, Table S5. Gene Ontology analysis of MYCN-regulated genes in Wilms' tumour.

Author Contributions: M.S.: conceptualization; methodology; formal analysis; investigation; validation; data curation; writing—original draft, review and editing; visualization and supervision. Z.M.: formal analysis, investigation and validation. J.B., J.H.P. and B.C.: investigation and validation. A.G.: visualization. D.C.: resources. K.M.: conceptualization; methodology; formal analysis; investigation; resources; funding acquisition; supervision; project administration; writing—original draft, review and editing; visualization. All authors have read and agreed to the published version of the manuscript.

Funding: The authors would like to thank the Children's Cancer and Leukaemia Group and Bethany's Wish (CCLGA 2017 01; CCLGA 2019 16), the Biotechnology and Biological Sciences Research Council (BB/P008232/1) and the Showering Fund for funding this study.

Institutional Review Board Statement: The study was conducted according to the guidelines of the Declaration of Helsinki, and approved by the East of England—Cambridgeshire and Hertfordshire Research Ethics Committee (18/EE/0350, 9/11/2018) and the Sydney Children's Hospital Network Human Research Ethics Committee (09/CHW/159 and LNR/14/SCHN/392).

Informed Consent Statement: All human tissues were acquired with appropriate local research ethics committee approval (see above).

Data Availability Statement: RNA sequencing data are available from the European Nucleotide Archive (ENA) under the accession number ERP125499.

Acknowledgments: The authors wish to thank Herman Yeger (University of Toronto) and Keith Brown (University of Bristol) for kindly sharing the WT cell-lines, Wit49 and 17.94, respectively. We also would like to thank Jane Coghill and Christy Waterfall at the University of Bristol Genomics Facility for assistance with transcriptomics and Andy Herman for help with flow cytometry. We are greatly indebted to Aysen Yuksei and Michael Krivanek for construction of the tissue microarrays and reviewing the pathology data.

Conflicts of Interest: The authors declare no conflict of interest. The funders had no role in the design of the study; in the collection, analyses, or interpretation of data; in the writing of the manuscript or in the decision to publish the results.

Abbreviations

ADMA	asymmetric di-methyl arginine
CM	condensing mesenchyme
DEG	differentially expressed genes
ECL	enhanced chemiluminescence
FACS	fluorescence-activated cell sorting
FDR	false discovery rate
FHWT	favourable histology Wilms' tumour
FK	fetal kidney
GO	Gene ontology
GSEA	Geneset enrichment analysis
HRP	horseradish peroxidase
IHC	immunohistochemistry
MNA	MYCN-amplified
NB	neuroblastoma
NES	normalised enrichment score
PTA	pre-tubular aggregates
R-Me	arginine methylation
SDMA	symmetric di-methyl arginine
TIM	translocase of the inner membrane
TMA	tissue microarray
TOM	translocase of the outer membrane
UB	ureteric bud
WT	Wilms' tumour

References

1. Green, D.M. Wilms' tumour. *Eur. J. Cancer* **1997**, *33*, 409–418.
2. Cotton, C.A.; Peterson, S.; Norkool, P.A.; Takashima, J.; Grigoriev, Y.; Green, D.M.; Breslow, N.E. Early and Late Mortality After Diagnosis of Wilms Tumor. *J. Clin. Oncol.* **2009**, *27*, 1304–1309, doi:10.1200/jco.2008.18.6981.
3. Pelletier, J.; Bruening, W.; Li, F.P.; Haber, D.A.; Glaser, T.; Housman, D.E. WT1 mutations contribute to abnormal genital system development and hereditary Wilms' tumour. *Nat. Cell Biol.* **1991**, *353*, 431–434, doi:10.1038/353431a0.
4. Pritchard-Jones, K.; Fleming, S.; Davidson, D.D.; Bickmore, W.; Porteous, D.; Gosden, C.; Bard, J.; Buckler, A.J.; Pelletier, J.; Housman, D.; et al. The candidate Wilms' tumour gene is involved in genitourinary development. *Nat. Cell Biol.* **1990**, *346*, 194–197, doi:10.1038/346194a0.
5. Bardeesy, N.; Falkoff, D.; Petruzzi, M.-J.; Nowak, N.J.; Zabel, B.; Adam, M.; Aguiar, M.C.; Grundy, P.; Shows, T.; Pelletier, J. Anaplastic Wilms' tumour, a subtype displaying poor prognosis, harbours p53 gene mutations. *Nat. Genet.* **1994**, *7*, 91–97, doi:10.1038/ng0594-91.
6. Koesters, R.; Ridder, R.; Kopp-Schneider, A.; Betts, D.; Adams, V.; Niggli, F.; Briner, J.; von Knebel Doeberitz, M. Mutational activation of the beta-catenin proto-oncogene is a common event in the development of Wilms' tumors. *Cancer Res.* **1999**, *59*, 3880–3882.
7. Torrezan, G.; Ferreira, E.N.; Nakahata, A.M.; Barros, B.D.F.; Castro, M.T.M.; Correa, B.R.; Krepischi, A.C.V.; Olivieri, E.H.R.; Cunha, I.W.; Tabori, U.; et al. Recurrent somatic mutation in DROSHA induces microRNA profile changes in Wilms tumour. *Nat. Commun.* **2014**, *5*, 4039, doi:10.1038/ncomms5039.

8. Rakheja, D.; Chen, K.S.; Liu, Y.; Shukla, A.A.; Schmid, V.; Chang, T.-C.; Khokhar, S.; Wickiser, J.E.; Karandikar, N.J.; Malter, J.S.; et al. Somatic mutations in DROSHA and DICER1 impair microRNA biogenesis through distinct mechanisms in Wilms tumours. *Nat. Commun.* **2014**, *5*, 4802, doi:10.1038/ncomms5802.
9. Wegert, J.; Ishaque, N.; Vardapour, R.; Georg, C.; Gu, Z.; Bieg, M.; Ziegler, B.; Bausenwein, S.; Nourkami, N.; Ludwig, N; et al. Mutations in the SIX1/2 Pathway and the DROSHA/DGCR8 miRNA Microprocessor Complex Underlie High-Risk Blastemal Type Wilms Tumors. *Cancer Cell* **2015**, *27*, 298–311.
10. Mahamdallie, S.S.; Hanks, S.; Karlin, K.L.; Zachariou, A.; Perdeaux, E.; Ruark, E.; Shaw, C.A.; Renwick, A.; Ramsay, E.; Yost, S.; et al. Mutations in the transcriptional repressor REST predispose to Wilms tumor. *Nat. Genet.* **2015**, *47*, 1471–1474, doi:10.1038/ng.3440.
11. Williams, R.D.; Al-Saadi, R.; Chagtai, T.; Popov, S.; Messahel, B.; Sebire, N.; Gessler, M.; Wegert, J.; Graf, N.; Leuschner, I.; et al. Subtype-Specific FBXW7 Mutation and MYCN Copy Number Gain in Wilms' Tumor. *Clin. Cancer Res.* **2010**, *16*, 2036–2045, doi:10.1158/1078-0432.ccr-09-2890.
12. Williams, R.D.; Al-Saadi, R.; Natrajan, R.; Mackay, A.; Chagtai, T.; Little, S.; Hing, S.N.; Fenwick, K.; Ashworth, A.; Grundy, P.; et al. Molecular profiling reveals frequent gain of MYCN and anaplasia-specific loss of 4q and 14q in wilms tumor. *Genes Chromosomes Cancer* **2011**, *50*, 982–995, doi:10.1002/gcc.20907.
13. Shaw, A.P.; Poirier, V.; Tyler, S.; Mott, M.; Berry, J.; Maitland, N.J. Expression of the N-myc oncogene in Wilms' tumour and related tissues. *Oncogene* **1988**, *3*, 143–149.
14. Zirn, B.; Hartmann, O.; Samans, B.; Krause, M.; Wittmann, S.; Mertens, F.; Graf, N.; Eilers, M.; Gessler, M. Expres-sion profiling of Wilms tumors reveals new candidate genes for different clinical parameters. International journal of cancer. *J. Int. Cancer* **2006**, *118*, 1954–1962.
15. Wittmann, S.; Wunder, C.; Zirn, B.; Furtwangler, R.; Wegert, J.; Graf, N.; Gessler, M. New prognostic markers re-vealed by evaluation of genes correlated with clinical parameters in Wilms tumors. *Genes Chromosomes Cancer* **2008**, *47*, 386–395.
16. Bates, C.M.; Kharzai, S.; Erwin, T.; Rossant, J.; Parada, L.F. Role of N-myc in the Developing Mouse Kidney. *Dev. Biol.* **2000**, *222*, 317–325, doi:10.1006/dbio.2000.9716.
17. Huang, M.; Weiss, W.A. Neuroblastoma and MYCN. *Cold Spring Harb. Perspect. Med.* **2013**, *3*, a014415, doi:10.1101/cshperspect.a014415.
18. Alami, J.; Williams, B.R.G.; Yeger, H. Derivation and characterization of a Wilms' tumour cell line, WiT 49. *Int. J. Cancer* **2003**, *107*, 365–374, doi:10.1002/ijc.11429.
19. Brown, K.W.; Charles, A.; Dallosso, A.R.; White, G.; Charlet, J.; Standen, G.R.; Malik, K. Characterization of 17.94, a novel anaplastic Wilms' tumor cell line. *Cancer Genet.* **2012**, *205*, 319–326, doi:10.1016/j.cancergen.2012.04.009.
20. Legge, D.; Li, L.; Moriarty, W.; Lee, D.; Szemes, M.; Zahed, A.; Panousopoulus, L.; Chung, W.Y.; Aghabi, Y.; Barratt, J.; et al. The epithelial splicing regulator ESRP2 is epigenetically repressed by DNA hypermethylation in Wilms tumour and acts as a tumour suppressor. *bioRxiv* **2020**, doi:10.1101/2020.11.02.364570.
21. Williams, R.D.; Chagtai, T.; Alcaide-German, M.; Apps, J.; Wegert, J.; Popov, S.; Vujanic, G.; Van Tinteren, H.; van de Heuvel-Eibrink, M.M.; Kool, M.; et al. Multiple mechanisms of MYCN dysregulation in Wilms tumour. *Oncotarget* **2015**, *6*, 7232–7243, doi:10.18632/oncotarget.3377.
22. Shoji, W.; Suenaga, Y.; Kaneko, Y.; Islam, S.M.; Alagu, J.; Yokoi, S.; Nio, M.; Nakagawara, A. NCYM promotes calpain-mediated Myc-nick production in human MYCN-amplified neuroblastoma cells. *Biochem. Biophys. Res. Commun.* **2015**, *461*, 501–506.
23. Wakamatsu, Y.; Watanabe, Y.; Shimono, A.; Kondoh, H. Transition of localization of the N-Myc protein from nucleus to cytoplasm in differentiating neurons. *Neuron* **1993**, *10*, 1–9, doi:10.1016/0896-6273(93)90236-k.
24. Beckers, A.; Van Peer, G.; Carter, D.R.; Gartlgruber, M.; Herrmann, C.; Agarwal, S.; Helsmoortel, H.H.; Althoff, K.; Molenaar, J.J.; Cheung, B.B.; et al. MYCN-driven regulatory mechanisms controlling LIN28B in neuroblastoma. *Cancer Lett.* **2015**, *366*, 123–132, doi:10.1016/j.canlet.2015.06.015.
25. Urbach, A.; Yermalovich, A.; Zhang, J.; Spina, C.S.; Zhu, H.; Perez-Atayde, A.R.; Shukrun, R.; Charlton, J.; Sebire, N.; Mifsud, W.; et al. Lin28 sustains early renal progenitors and induces Wilms tumor. *Genes Dev.* **2014**, *28*, 971–982, doi:10.1101/gad.237149.113.
26. Yermalovich, A.V.; Osborne, J.K.; Sousa, P.; Han, A.; Kinney, M.A.; Chen, M.J.; Robinton, D.A.; Montie, H.; Pearson, D.S.; Wilson, S.B.; et al. Lin28 and let-7 regulate the timing of cessation of murine nephrogenesis. *Nat. Commun.* **2019**, *10*, 168, doi:10.1038/s41467-018-08127-4.
27. Tsialikas, J.; Romer-Seibert, J. LIN28: Roles and regulation in development and beyond. *Development* **2015**, *142*, 2397–2404, doi:10.1242/dev.117580.
28. Blockus, H.; Chédotal, A. Slit-Robo signaling. *Development* **2016**, *143*, 3037–3044, doi:10.1242/dev.132829.
29. Xian, J.; Aitchison, A.; Bobrow, L.; Corbett, G.; Pannell, R.; Rabbitts, T.; Rabbitts, P. Targeted disruption of the 3p12 gene, Dutt1/Robo1, predisposes mice to lung adenocarcinomas and lymphomas with methylation of the gene promoter. *Cancer Res.* **2004**, *64*, 6432–6437.
30. Grieshammer, U.; Le, M.; Plump, A.S.; Wang, F.; Tessier-Lavigne, M.; Martin, G.R. SLIT2-mediated ROBO2 signal-ing restricts kidney induction to a single site. *Dev. Cell* **2004**, *6*, 709–717.
31. Piper, M.; Georgas, K.; Yamada, T.; Little, M. Expression of the vertebrate Slit gene family and their putative receptors, the Robo genes, in the developing murine kidney. *Mech. Dev.* **2000**, *94*, 213–217.

32. Astuti, D.; Da Silva, N.F.; Dallol, A.; Gentle, D.; Martinsson, T.; Kogner, P.; Grundy, R.; Kishida, T.; Yao, M.; Latif, F.; et al. SLIT2 promoter methylation analysis in neuroblastoma, Wilms' tumour and renal cell carcinoma. *Br. J. Cancer* **2004**, *90*, 515–521, doi:10.1038/sj.bjc.6601447.
33. Menon, R.; Otto, E.A.; Kokoruda, A.; Zhou, J.; Zhang, Z.; Yoon, E.; Chen, Y.-C.; Troyanskaya, O.; Spence, J.R.; Kretzler, M.; et al. Single-cell analysis of progenitor cell dynamics and lineage specification in the human fetal kidney. *Development* **2018**, *145*, dev164038, doi:10.1242/dev.164038.
34. Fan, R.; Grignon, D.; Gulcicek, E.E.; Faught, P.; Cheng, L. Proteomic studies of Anaplasia in Wilms Tumor. *Proteom. Insights* **2011**, *4*, PRI.S7466–35, doi:10.4137/pri.s7466.
35. Valentijn, L.J.; Koster, J.; Haneveld, F.; Aissa, R.A.; Van Sluis, P.; Broekmans, M.E.C.; Molenaar, J.J.; Van Nes, J.; Versteeg, R. Functional MYCN signature predicts outcome of neuroblastoma irrespective of MYCN amplification. *Proc. Natl. Acad. Sci. USA* **2012**, *109*, 19190–19195, doi:10.1073/pnas.1208215109.
36. Boon, K.; Caron, H.N.; van Asperen, R.; Valentijn, L.; Hermus, M.C.; van Sluis, P.; Roobeek, I.; Weis, I.; Voute, P.A.; Schwab, M.; et al. N-myc enhances the expression of a large set of genes functioning in ribosome biogenesis and protein syn-thesis. *EMBO J.* **2001**, *20*, 1383–1393.
37. Hsu, C.-L.; Chang, H.-Y.; Chang, J.-Y.; Hsu, W.-M.; Huang, H.-C.; Juan, H.-F. Unveiling MYCN regulatory networks in neuroblastoma via integrative analysis of heterogeneous genomics data. *Oncotarget* **2016**, *7*, 36293–36310, doi:10.18632/oncotarget.9202.
38. Li, C.M.; Kim, C.E.; Margolin, A.A.; Guo, M.; Zhu, J.; Mason, J.M.; Hensle, T.W.; Murty, V.V.; Grundy, P.E.; Fearon, E.R.; et al. CTNNB1 mutations and overexpression of Wnt/beta-catenin target genes in WT1-mutant Wilms' tumors. *Am. J. Pathol.* **2004**, *165*, 1943–1953.
39. Liberzon, A.; Birger, C.; Thorvaldsdottir, H.; Ghandi, M.; Mesirov, J.P.; Tamayo, P. The Molecular Signatures Database (MSigDB) hallmark gene set collection. *Cell Syst.* **2015**, *1*, 417–425.
40. Montemurro, L.; Raieli, S.; Angelucci, S.; Bartolucci, D.; Amadesi, C.; Lampis, S.; Scardovi, A.L.; Venturelli, L.; Nieddu, G.; Cerisoli, L.; et al. A Novel MYCN-Specific Antigene Oligonucleotide Deregulates Mitochondria and Inhibits Tumor Growth in MYCN-Amplified Neuroblastoma. *Cancer Res.* **2019**, *79*, 6166–6177, doi:10.1158/0008-5472.can-19-0008.
41. Hald, O.H.; Olsen, L.; Gallo-Oller, G.; Elfman, L.H.M.; Løkke, C.; Kogner, P.; Sveinbjörnsson, B.; Flægstad, T.; Johnsen, J.I.; Einvik, C. Inhibitors of ribosome biogenesis repress the growth of MYCN-amplified neuroblastoma. *Oncogene* **2019**, *38*, 2800–2813, doi:10.1038/s41388-018-0611-7.
42. Zhang, S.; Wei, J.S.; Li, S.Q.; Badgett, T.C.; Song, Y.K.; Agarwal, S.; Coarfa, C.; Tolman, C.; Hurd, L.; Liao, H.; et al. MYCN controls an alternative RNA splicing program in high-risk metastatic neuroblastoma. *Cancer Lett.* **2016**, *371*, 214–224, doi:10.1016/j.canlet.2015.11.045.
43. Oliynyk, G.; Ruiz-Pérez, M.V.; Sainero-Alcolado, L.; Dzieran, J.; Zirath, H.; Gallart-Ayala, H.; Wheelock, C.E.; Johansson, H.J.; Nilsson, R.; Lehtiö, J.; et al. MYCN-enhanced Oxidative and Glycolytic Metabolism Reveals Vulnerabilities for Targeting Neuroblastoma. *iScience* **2019**, *21*, 188–204, doi:10.1016/j.isci.2019.10.020.
44. Viswanathan, S.R.; Powers, J.T.; Einhorn, W.; Hoshida, Y.; Ng, T.L.; Toffanin, S.; O'Sullivan, M.; Lu, J.; Phillips, L.A.; Lockhart, V.L.; et al. Lin28 promotes transformation and is associated with advanced human malignancies. *Nat. Genet.* **2009**, *41*, 843–848, doi:10.1038/ng.392.
45. Pfanner, N.; Meijer, M. The Tom and Tim machine. *Curr. Biol.* **1997**, *7*, R100–R103.
46. Dang, C.V.; Le, A.; Gao, P. MYC-Induced Cancer Cell Energy Metabolism and Therapeutic Opportunities. *Clin. Cancer Res.* **2009**, *15*, 6479–6483, doi:10.1158/1078-0432.ccr-09-0889.
47. Huang, C.-C.; Gadd, S.; Breslow, N.; Cutcliffe, C.; Sredni, S.T.; Helenowski, I.B.; Dome, J.S.; Grundy, P.E.; Green, D.M.; Fritsch, M.K.; et al. Predicting Relapse in Favorable Histology Wilms Tumor Using Gene Expression Analysis: A Report from the Renal Tumor Committee of the Children's Oncology Group. *Clin. Cancer Res.* **2009**, *15*, 1770–1778, doi:10.1158/1078-0432.ccr-08-1030.
48. Gadd, S.; Huff, V.; Huang, C.-C.; Ruteshouser, E.C.; Dome, J.S.; Grundy, P.E.; Breslow, N.; Jennings, L.; Green, D.M.; Beckwith, J.B.; et al. Clinically Relevant Subsets Identified by Gene Expression Patterns Support a Revised Ontogenic Model of Wilms Tumor: A Children's Oncology Group Study. *Neoplasia* **2012**, *14*, 742–IN21, doi:10.1593/neo.12714.
49. Park, S.-H.; Lee, A.-R.; Choi, K.; Joung, S.; Yoon, J.-B.; Kim, J.S. TOMM20 as a potential therapeutic target of colorectal cancer. *BMB Rep.* **2019**, *52*, 712–717, doi:10.5483/bmbrep.2019.52.12.249.
50. Roche, M.E.; Lin, Z.; Whitaker-Menezes, D.; Zhan, T.; Szuhai, K.; Bovee, J.V.; Abraham, J.A.; Jiang, W.; Martinez-Outschoorn, U.; Basu-Mallick, A. Translocase of the outer mitochondrial membrane complex subunit 20 (TOMM20) facilitates cancer aggressiveness and therapeutic resistance in chondrosarcoma. *Biochim. Biophys. Acta (BBA) Mol. Basis Dis.* **2020**, *1866*, 165962, doi:10.1016/j.bbadis.2020.165962.
51. Feichtinger, R.G.; Neureiter, D.; Royer-Pokora, B.; Mayr, J.A.; Zimmermann, F.A.; Jones, N.; Koegler, C.; Ratschek, M.; Sperl, W.; Kofler, B. Heterogeneity of mitochondrial energy metabolism in classical triphasic Wilms' tumor. *Front Biosci.* (*Elite Ed*) **2011**, *3*, 187–193.
52. Terada, K.; Kanazawa, M.; Yano, M.; Hanson, B.; Hoogenraad, N.; Mori, M. Participation of the import receptor Tom20 in protein import into mammalian mitochondria: Analyses in vitro and in cultured cells. *FEBS Lett.* **1997**, *403*, 309–312, doi:10.1016/s0014-5793(97)00070-7.

53. Westermann, F.; Muth, D.; Benner, A.; Bauer, T.; Henrich, K.O.; Oberthuer, A.; Brors, B.; Beissbarth, T.; Vandesompele, J.; Pattyn, F.; et al. Distinct transcriptional MYCN/c-MYC activities are associated with spontaneous regression or ma-lignant progression in neuroblastomas. *Genome Biol*. **2008**, *9*, R150.
54. Yang, Y.; Bedford, M.T. Protein arginine methyltransferases and cancer. *Nat. Rev. Cancer* **2012**, *13*, 37–50, doi:10.1038/nrc3409.
55. Park, J.H.; Szemes, M.; Vieira, G.C.; Melegh, Z.; Malik, S.; Heesom, K.J.; Von Wallwitz-Freitas, L.; Greenhough, A.; Brown, K.W.; Zheng, Y.G.; et al. Protein arginine methyltransferase 5 is a key regulator of the MYCN oncoprotein in neuro-blastoma cells. *Mol. Oncol*. **2015**, *9*, 617–627.
56. Hua, Z.-Y.; Hansen, J.N.; He, M.; Dai, S.-K.; Choi, Y.; Fulton, M.D.; Lloyd, S.M.; Szemes, M.; Sen, J.; Ding, H.-F.; et al. PRMT1 promotes neuroblastoma cell survival through ATF5. *Oncogenesis* **2020**, *9*, 1–12, doi:10.1038/s41389-020-0237-9.
57. Chan-Penebre, E.; Kuplast, K.G.; Majer, C.R.; Boriack-Sjodin, P.A.; Wigle, T.J.; Johnston, L.D.; Rioux, N.; Munchhof, M.J.; Jin, L.; Jacques, S.L.; et al. A selective inhibitor of PRMT5 with in vivo and in vitro potency in MCL models. *Nat. Chem. Biol.* **2015**, *11*, 432–437, doi:10.1038/nchembio.1810.
58. Fedoriw, A.; Rajapurkar, S.R.; O'Brien, S.; Gerhart, S.V.; Mitchell, L.H.; Adams, N.D.; Rioux, N.; Lingaraj, T.; Ribich, S.A.; Pappalardi, M.B.; et al. Anti-tumor Activity of the Type I PRMT Inhibitor, GSK3368715, Synergizes with PRMT5 Inhibition through MTAP Loss. *Cancer Cell* **2019**, *36*, 100–114.e25
59. Siu, L.; Rasco, D.; Vinay, S.P.; Romano, P.M.; Menis, J.; Opdam, F.; Heinhuis, K.; Egger, J.; Gorman, S.; Parasrampuria, R.; et al. METEOR-1: A phase I study of GSK3326595, a first-in-class protein arginine methyltransferase 5 (PRMT5) inhibitor, in advanced solid tumours. *Ann. Oncol.* **2019**, *30*, v159, doi:10.1093/annonc/mdz244.
60. Ooi, L.; Wood, I.C. Chromatin crosstalk in development and disease: Lessons from REST. *Nat. Rev. Genet.* **2007**, *8*, 544–554, doi:10.1038/nrg2100.
61. Satoh, J.; Kawana, N.; Yamamoto, Y. ChIP-Seq Data Mining: Remarkable Differences in NRSF/REST Target Genes between Human ESC and ESC-Derived Neurons. *Bioinform. Biol. Insights* **2013**, *7*, 357–368.
62. Johnson, R.; Teh, C.H.-L.; Kunarso, G.; Wong, K.Y.; Srinivasan, G.; Cooper, M.L.; Volta, M.; Chan, S.S.-L.; Lipovich, L.; Pollard, S.M.; et al. REST regulates distinct transcriptional networks in embryonic and neural stem cells. *PLoS Biol.* **2008**, *6*, e256, doi:10.1371/journal.pbio.0060256.